

## Otherwise identical particles with differing, fixed speeds demix under time-reversible dynamics

G. Baglietto and A. Seif<sup>1</sup>

*Instituto de Física de Líquidos y Sistemas Biológicos (IFLYSIB), CONICET y Universidad Nacional de La Plata, Calle 59 No. 789, B1900BTE La Plata, Argentina and CCT CONICET La Plata, Consejo Nacional de Investigaciones Científicas y Técnicas, Argentina*

T. S. Grigera

*Instituto de Física de Líquidos y Sistemas Biológicos (IFLYSIB), CONICET y Universidad Nacional de La Plata, Calle 59 No. 789, B1900BTE La Plata, Argentina; CCT CONICET La Plata, Consejo Nacional de Investigaciones Científicas y Técnicas, Argentina; and Departamento de Física, Facultad de Ciencias Exactas, Universidad Nacional de La Plata, Argentina*

W. Paul<sup>2</sup>\*

*Institute of Physics, Martin-Luther University Halle-Wittenberg, 06099 Halle, Germany*



(Received 20 December 2019; accepted 26 May 2020; published 18 June 2020)

In recent years situations where otherwise identical particles demix when different degrees of freedom do not thermalize have become a research focus in nonequilibrium statistical mechanics. The majority of these models are formulated in the context of active particles, but the phenomenon also occurs for particles without driving. All the models studied so far share the property that they do not obey microscopic reversibility, and it may be thought that this is a necessary condition for such demixing to occur. We show here that such a demixing transition also occurs in a mixture of otherwise identical particles moving at two fixed but different speeds according to a time-reversible quasi-Newtonian dynamics. The mechanical instability underlying this behavior is generated by the lack of thermalization between the two subsystems, which is shared by all systems showing this behavior.

DOI: [10.1103/PhysRevE.101.062606](https://doi.org/10.1103/PhysRevE.101.062606)

### I. INTRODUCTION

Active particles have been a topic of prominence in nonequilibrium statistical mechanics for quite some time now [1–4] due to the occurrence of nonequilibrium phase transitions in these systems. One fascinating finding is the existence of a motility-induced condensation transition [termed motility-induced phase separation (MIPS)] of identical hard particles [3]. This has been studied in detail for active Brownian spheres [5–8] and also for active Brownian disks [6,9–14] but also considered for systems including polar interactions [15]. Experimentally, it is not easy to access the phase-separated state [16,17], but the prediction for a precursor of the phase separation, the cluster phase, where one observes local phase separation, has been verified [18,19]. Furthermore, a motility-induced phase separation of a mixture of active and passive Brownian particles [20] has been identified.

While the motivation for the study of these active systems often came from complex biological phenomena, much effort has been devoted to clarify how much of this complex phenomenology can already be understood based on the nonequilibrium statistical mechanics of idealized physical models. From this it has been understood that the phase transitions occur when a particle-based Péclet number (the ratio of rotational time scale to the time it takes to advectively traverse a particle diameter) becomes large enough. Advective

translational motion is much faster than diffusive orientational motion. When particles collide to form clusters, the desorption rate from the cluster becomes smaller than the adsorption rate from the environment until a stationary cluster size is reached, which can be a completely demixed system. The stationary behavior is thus interface controlled [21], in contrast to the equilibrium phase transitions which are controlled by bulk free energies. The particles in the dense cluster are effectively slowed down compared to those in the surrounding fluid, so that their kinetic pressure is smaller than in the surrounding fluid. Mechanical equilibrium requires this to be compensated by a higher density of the cluster.

One ingredient shared by all these studies is that systems of active particles do not obey microscopic reversibility in their dynamic equations, and one might think that this is essential for the phenomenology to be observed. In the work of Klamser *et al.* [14], the group introduced moves breaking microscopic reversibility into a Monte Carlo procedure they had employed before to determine the two-dimensional phase behavior of passive repulsive disks [22]. They showed that they could introduce MIPS into their model in this way.

Another model system which also follows a nonreversible Langevin dynamics was studied by Weber *et al.* [23]. It consists of a binary mixture of passive particles, which, however, differ only in their diffusivities, while their size, mass, and interaction potential are identical. The diffusivities govern the strength of the stochastic forces in the model. Different diffusivities can also be interpreted as different kinetic temperatures leading to different kinetic pressures. This again leads

\*Wolfgang.Paul@Physik.Uni-Halle.De

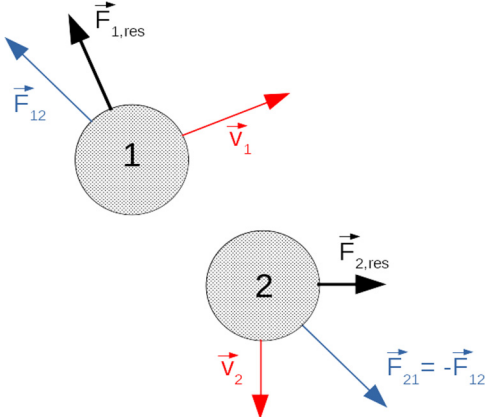


FIG. 1. Schematics of a binary collision. The conservative forces (blue) obey Newton's third law; the resulting forces after the projection on the respective velocities has been subtracted do not.

to a mechanical instability, cluster formation, and, ultimately, demixing for large enough diffusivity ratio.

Our model is in spirit similar to that of Ref. [23]; however, we will be looking at a modified Newtonian dynamics which keeps its time reversibility. We will show that the phenomenology of our model is very similar to what is observed by Weber *et al.*, so that we can conclude that breaking of microscopic reversibility is not a necessary ingredient for phase segregation to occur in systems where only the momentum space properties of the particles differ.

## II. MODEL

We are suggesting a minimal model obeying quasi-Newtonian dynamics. We require the speed (i.e., the modulus of the velocity) of all particles to be fixed at all times and thus modify Newton's equation to only contain that part of the force on the particle which is perpendicular to the instantaneous velocity of the particle:

$$\begin{aligned}\dot{\vec{r}}_i(t) &= \vec{v}_i(t) \\ m\dot{\vec{v}}_i(t) &= \vec{F}_i(t) - (\vec{F}_i(t) \cdot \hat{e}_i(t))\hat{e}_i(t).\end{aligned}\quad (1)$$

Here we define  $\vec{v}_i(t) = v_i \hat{e}_i(t)$ , so we subtract the projection onto the velocity direction  $\hat{e}_i(t)$  from the total force on particle  $i$ ,  $\vec{F}_i(t)$ , which we assume to be given by pairwise interactions,  $\vec{F}_i(t) = \sum_{j \neq i} \vec{F}_{ij}(t)$ . For simplicity, we set all particle masses equal,  $m_i = m$ . A binary collision is schematically shown in Fig. 1.

This modified Newton equation retains the time-reversal symmetry of the original equation, but each collision violates energy, momentum, and angular momentum conservation during the collision duration. The forces also do not obey Newton's third law. (Barberis and Peruani mention this fact for an active model they were using [24]). We choose in the following a two-dimensional system of particles interacting through a Weeks-Chandler-Anderson (WCA) potential

$$U(r) = \begin{cases} 4\varepsilon \left[ \left( \frac{\sigma}{r} \right)^{12} - \left( \frac{\sigma}{r} \right)^6 \right] + \varepsilon, & r \leq 2^{1/6}\sigma \\ 0, & r > 2^{1/6}\sigma \end{cases}. \quad (2)$$

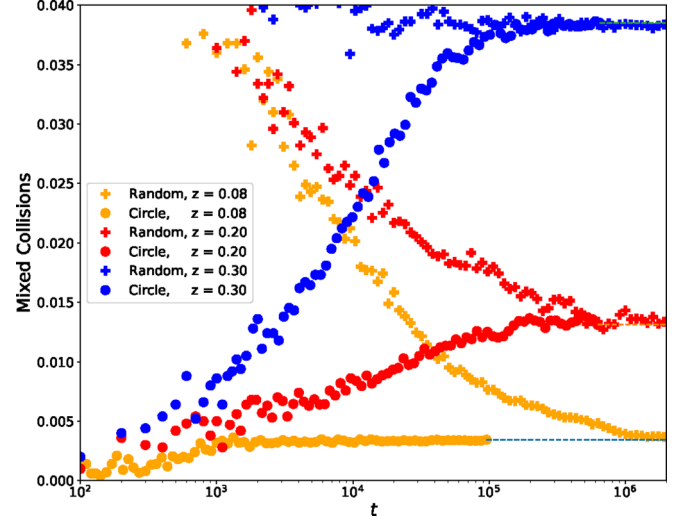


FIG. 2. Fraction of slow-fast interparticle collisions as a function of time for different speed ratios and starting from different initial configurations as indicated in the legend.

Here  $\sigma$  is the diameter of the disks,  $\varepsilon$  the strength of the interaction, and we cut off the interaction at the position of the minimum of the potential and shift it to zero. With this finite range potential it is easy to see that energy conservation holds asymptotically in sufficiently dilute systems for each collision, as then the total energy before and after the collision is just given by the kinetic energy of the particles which is fixed by construction. In a dense system, like we will study here, this is no longer the case. Asymptotic conservation for each individual collision does not hold for linear and angular momenta, independent of density. However, due to the time inversion symmetry of the collisions and the fact that forward and backward collision occur with the same probability, the total energy and linear and angular momenta of the system are conserved on average, also in dense systems. Thus even though the system is open, it does not gain energy or linear and angular momentum in its time evolution and does not need any thermostatization to counteract such an instability.

For the simulation, we choose Lennard-Jones units, which amounts to setting  $m$ ,  $\sigma$ , and  $\varepsilon$  equal to unity in the above equations and measuring time in units of  $\tau = \sqrt{m\sigma^2/\varepsilon}$ . Using this model, we study a mixture of  $N = 1000$  particles in a simulation box with side length  $L = 40$  using periodic boundary conditions and with two different velocities, a fraction of  $fN$  fast particles with  $v_i = v_f$  and  $(1-f)N$  slow particles with  $v_i = v_s$ . We will show that such a mixture exhibits phase separation of the slow and fast particles when one decreases the speed ratio  $z = v_s/v_f$  between them.

We will discuss below that our mixture of particles with two different fixed velocities is mechanically unstable against demixing. This instability leads to the development of a stationary interface size between the cluster(s) of fast and slow particles, respectively, which gives rise to a stationary number of collisions between the two types of particles. We observe how this stationary state is reached from different starting conditions to determine the equilibration in our system, as shown in Fig. 2. All statistical analysis is performed only after

a stationary behavior of the number of slow-fast collisions has been reached.

### III. RESULTS

To understand the phase behavior of the system we analyze the virial equation for the hydrostatic pressure [9,25,26]. Although the system does not thermalize the slow and the fast particles and thus it is not obvious whether this pressure can be defined as the thermodynamic derivative of a free energy [21], its mechanical definition is still applicable, and any possible coexisting phases need to exhibit at least mechanical equilibrium. For an  $N$ -particle system in an area  $A$  we have

$$p = \frac{1}{A} \left\langle \sum_{i=1}^N \frac{1}{2} \vec{v}_i^2 \right\rangle_{neq} + \frac{1}{2A} \left\langle \sum_{i=1}^N \vec{r}_i \cdot [\vec{F}_i - (\vec{F}_i \cdot \hat{e}_i) \hat{e}_i] \right\rangle_{neq}. \quad (3)$$

The average is taken over an unknown nonequilibrium probability distribution on the phase space of this system. The model has no polar interactions between the velocities as would be typical for flocking models like, e.g., the Vicsek model, so we can assume the distribution in velocity space to be uniform on the circle for every particle. With this assumption we can perform the average over the velocity distribution in the last term in Eq. (3):

$$\frac{1}{2\pi} \int_0^{2\pi} \langle (\vec{r}_i \vec{F}_i)(\hat{e}_i \hat{e}_i) \rangle = \frac{1}{2} \vec{r}_i \cdot \vec{F}_i. \quad (4)$$

By using only the component of the force perpendicular to the velocities, we reduce their contribution to the excess pressure by a factor of 2 and obtain

$$p = \frac{1}{A} \sum_{i=1}^N \frac{1}{2} \vec{v}_i^2 + \frac{1}{4A} \left\langle \sum_{i=1}^N \vec{r}_i \cdot \vec{F}_i \right\rangle_{neq,\vec{r}}, \quad (5)$$

where the average only has to be performed over the spatial part of the unknown nonequilibrium distribution. Except for the change of distribution, this is the virial pressure of a system of WCA disks at an effective temperature  $k_B T_{\text{eff}} = 1/2N \sum_i v_i^2$  and an interaction reduced by a factor of 2. We can thus expect the nonequilibrium distribution for this system to be close to the canonical equilibrium distribution for a system with this effective temperature. The pure system then can be assumed to have the same phase behavior as the standard WCA disks, exhibiting a fluid, a hexatic, and a solid phase [14]. When we consider a mixture as defined above in its homogeneous state, we obtain

$$p = \frac{1}{2A} [N_f v_f^2 + N_s v_s^2] + \frac{1}{4A} \left\langle \sum_{i=1}^N \vec{r}_i \cdot \vec{F}_i \right\rangle_{neq,\vec{r}}, \quad (6)$$

the force contribution being equal between the two species. However, such a system can phase separate into a dense phase of slow particles and a less dense phase of fast particles, where the difference in kinetic pressure in the two phases is balanced by a difference in force contribution due to the different densities. When the  $N_f = Nf$  fast particles take up a fraction  $xA$  of the total area and the  $N_s = N(1-f)$  slow particles in the area  $(1-x)A$  we have the following condition

for mechanical equilibrium:

$$\begin{aligned} & \frac{f\rho v_f^2}{2x} + \frac{1}{4xA} \left\langle \sum_{i=1}^{N_f} \vec{r}_i \cdot \vec{F}_i \right\rangle_{neq,\vec{r}} \\ &= \frac{(1-f)\rho v_s^2}{2(1-x)} + \frac{1}{4(1-x)A} \left\langle \sum_{i=1}^{N_s} \vec{r}_i \cdot \vec{F}_i \right\rangle_{neq,\vec{r}}. \end{aligned} \quad (7)$$

The phase separation mechanism thus is similar to the model in [23] and also to active particles, where in the overdamped case the difference in the kinetic contribution to the pressure is created by a density-dependent reduction in the speed compared to the active driving speed [3,7,9]. Accounting for the inertia of active particles, it was recently shown that this leads to liquid-gas coexistence at differing temperatures [27].

Using the close similarity of the homogeneous system to the standard WCA disks, we can assume the existence of a virial expansion

$$\frac{p_f}{\rho_f v_f^2 / 2} = 1 + \frac{1}{2} \sum_n B_n \left( \frac{\rho_f}{\rho_0} \right)^{n-1}, \quad (8)$$

where we kept the prefactor 1/2 in front of the sum, so that the virial coefficients reduce to the standard ones when we turn off the force constraints. The virial coefficient will in general depend on temperature in equilibrium (here on the chosen speed of the particles). We also normalized the density by the closed-packed density of hard disks,  $\rho_0 = \sqrt{2/3}$ . A similar relation can be written down for the  $(1-f)N$  slow particles occupying a fraction  $(1-x)A$  of the total area and, of course, for the mixed system, also. Inserting this into Eq. (7) and dividing by the kinetic pressure contribution of the fast particles we obtain

$$\begin{aligned} & \frac{f}{x} \left[ 1 + \frac{1}{2} \sum_{n=2}^{\infty} B_n \left( \frac{f\rho}{x\rho_0} \right)^{n-1} \right] \\ &= \frac{1-f}{(1-x)} z^2 \left[ 1 + \frac{1}{2} \sum_{n=2}^{\infty} B_n \left( \frac{(1-f)\rho}{(1-x)\rho_0} \right)^{n-1} \right], \end{aligned} \quad (9)$$

with the control parameter  $z = v_s/v_f$ . Local concentration fluctuations lead to a mechanical instability against demixing as soon as  $z < 1$ . Fixing the control parameter  $z$ , this equation determines the area fractions of slow and fast particles, and with that their respective densities for every given average density  $\rho$  and fraction of fast particles  $f$ . The fact that the kinetic pressure in the two subsystems never equilibrates enforces a phase separation into a less dense phase of fast particles and a denser phase of slow particles to counteract this pressure difference.

We want to apply this theoretical description to computer simulations of a mixed system with fraction  $f = 1/2$  at density  $\rho = 0.49$ . We performed molecular dynamics simulations of Eq. (1) and made sure the system found the same stationary state from different starting conditions. In Fig. 3 we show a sequence of configuration snapshots for different values of  $z < 1$ . Obviously, even for  $z = 0.8$  there exists a local phase separation (cluster phase) between the two species. For smaller  $z$ , the species aggregate into two separated domains. When the slow domain is large enough to be able to percolate

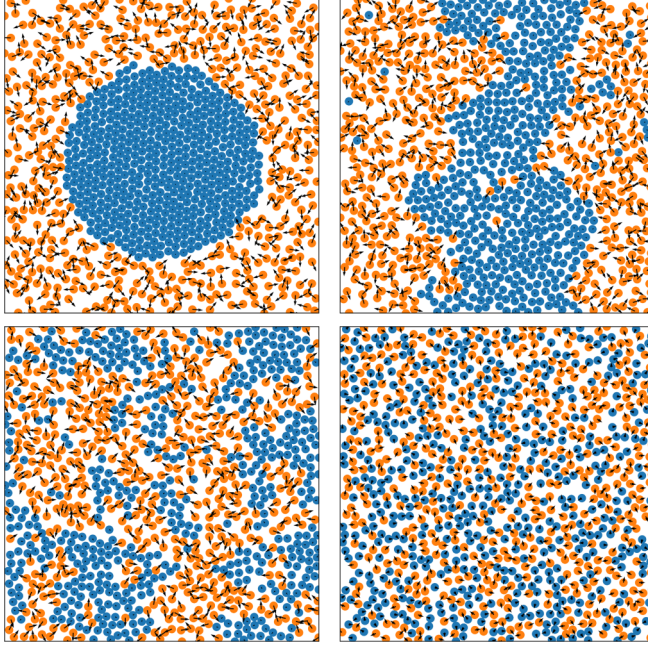


FIG. 3. Snapshots of particle configurations at density  $\rho = 0.49$ , mixing ratio  $f = 0.5$ , and fast particle speed  $v_f = 0.1$ . The different panels are for  $z = 0.05$  (upper left),  $z = 0.19$  (upper right),  $z = 0.25$  (lower left), and  $z = 0.8$  (lower right).

( $z = 0.19$ ) in the finite size system, we observe a strip geometry (influenced by finite size effects). For still smaller  $z$  the slow domain becomes circular and reaches sufficiently high density to exhibit hexagonal order ( $z = 0.05$ ).

To quantify the demixing instability predicted by Eq. (7), one can use a Voronoi tessellation of the system (shown exemplary in the inset of Fig. 4) and determine the combined areas of the Voronoi cells of each species. For a homogeneously mixed system of equal composition, these equal half the system size and both species have the same areal density.

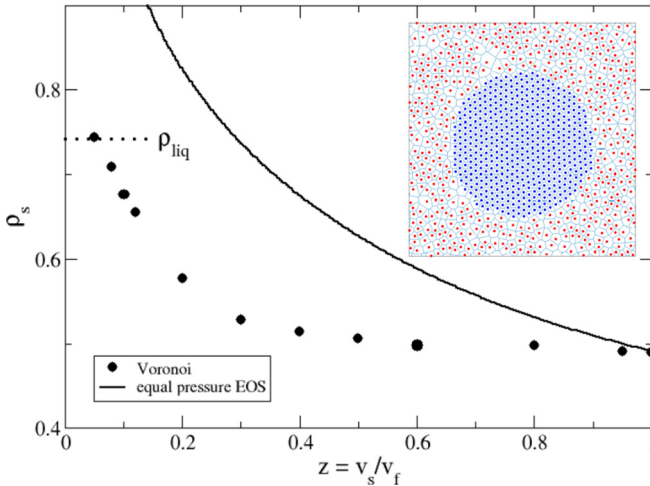


FIG. 4. Density of the slow component  $\rho_s = N_s/(1 - x)A$  with the area given by the combined areas of the individual Voronoi cells (see inset for  $z = 0.05$ ). Data points are from the simulation, the curve is from a theoretical prediction discussed in the text.

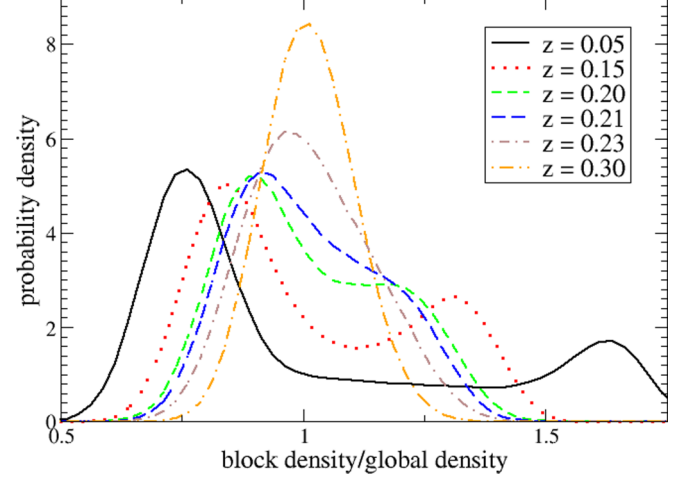


FIG. 5. Sub-block analysis of the local density distribution for a linear block size  $b = 5$ . At larger  $z$  the distribution is unimodal with a peak at the average density; at smaller  $z$  a coexistence between high-density boxes (slow particles) and low-density boxes (fast particles) develops.

In Fig. 4 the areal density as a function of the velocity ratio  $z$  is shown by the symbols. To get a qualitative prediction for the increase of the density of clusters of slow particles upon reduction of  $z$ , we use a phenomenological formulation of the equation of state (EOS) of hard disks presented by Woodcock [28] and based on the virial coefficients determined in [29]. For the fast particles this reads

$$\frac{p_f}{\rho_f v_f^2 / 2} = 1 + \frac{1}{2} \sum_{n=2}^{11} B_n \left( \frac{\rho_f}{\rho_0} \right)^{n-1} + \frac{\rho}{\rho_0} \left[ \frac{4.262}{1 - \rho/\rho_0} - \frac{0.1125}{(1 - \rho/\rho_0)^2} \right], \quad (10)$$

and for slow particles the corresponding equation holds. Inserting the EOS Eq. (10) into the requirement of mechanical equilibrium Eq. (9) and assuming the hard disk virial coefficients of [28] to be a reasonable approximation of the EOS of the pure systems of slow and fast WCA disks, respectively, we can solve for a prediction of the areal density of slow particles, which is shown as the continuous line in Fig. 4. As stated before, the system is mechanically unstable against demixing as soon as  $z < 1$ , which is shown both by the simulation and the theory. This qualitative feature agrees between theory and simulation; however, quantitatively, the use of the hard disk virial coefficients is, of course, an oversimplification. The theoretical curve thus increases much faster than the simulation result.

While the system is unstable against demixing as soon as  $z < 1$ , there is a threshold for macroscopic demixing into a compact phase of slow particles at higher density than the average one, embedded into a phase of fast particles at a reduced density. To locate this transition we use the sub-block analysis [30] exhibited for the local density in Fig. 5, which shows the density distribution observed in sub-blocks of size  $b = 5$  for different choices of  $z$ . Clearly, at small  $z$  a bimodal

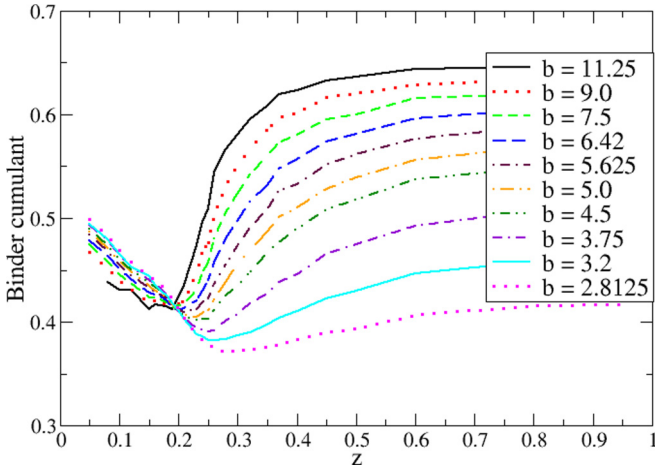


FIG. 6. Fourth-order cumulant of the block molar concentration of the fast particles for different block sizes indicated in the legend.

distribution develops indicative of the demixing into a dense phase of slow particles and a dilute phase of fast particles.

For the density, however, we basically have the equivalent of a field-driven phase separation, as the mechanical instability shows, so we have to look for a different order parameter. We find the clearest signature of a phase transition when we look at the fourth order cumulant of the local molar concentration of the fast particles  $c_b = N_{f,b}/(N_{f,b} + N_{s,b}) = \rho_{f,b}/(\rho_{f,b} + \rho_{s,b})$  shown in Fig. 6. There is a low temperature intersection point of the cumulants at around  $z \simeq 0.19$ ; however, the minimum occurring in these cumulants is indicative for a first order phase transition. The location of this thermodynamic transition is obtained by extrapolating the positions of the minima to infinite block size, as done in Fig. 7. It is noteworthy that the positions of the minima do not scale with the square of the inverse block length (the inverse volume predicted by the scaling theory for first order phase transitions) but with its first power. We think this is due to the fact that in the molar concentration both the numerator and denominator are fluctuating quantities. The extrapolation

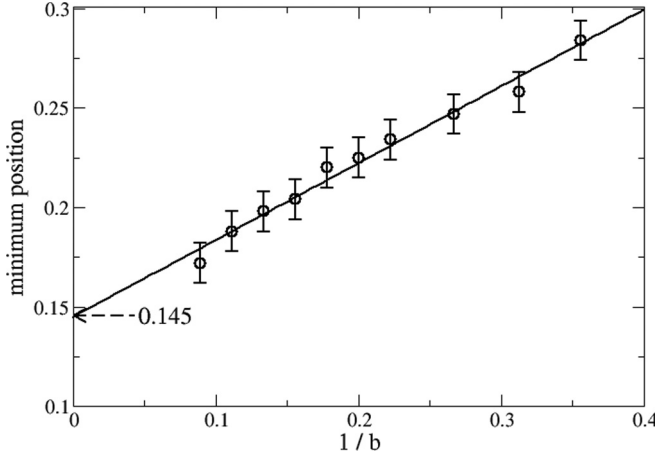


FIG. 7. Extrapolation of the positions of the minima in Fig. 6 to infinite sub-block size. The scaling is linear in the inverse of the sub-block size  $b$ .

converges to  $z_c = 0.145$  for the macroscopic demixing of the two species. Below this value the system thus exhibits macroscopic demixing into a liquid phase of slow particles and a gas phase of fast particles. The liquid phase gets further compressed upon reduction of  $z$ , bringing it into the realm of the two-dimensional liquid-hexatic transition (see Fig. 4).

Recently Hajibabaei and Kim [31] examined the melting scenario of two-dimensional WCA liquids in detail, paying special attention to the influence of temperature on the phase behavior. Temperature is part of the EOS of the system, so the virial coefficients we use in Eq. (10) are temperature dependent. Hajibabaei and Kim show that the Kosterlitz-Thouless-Halperin-Nelson-Young (KTHNY) melting scenario is observed for temperatures  $T > 1.1$  in Lennard-Jones units, but below  $T = 0.7$  there is a first order transition between a liquid and a hexagonally ordered solid with long-range orientational and positional correlations. When we translate the fixed kinetic energy of our slow particles into an equivalent temperature, we are working in the regime  $T < 10^{-3}$ . We extrapolated the limiting liquid density at the liquid-solid coexistence of Ref. [31] to this temperature range (the data allow for a simple linear extrapolation) and obtained a liquid density at coexistence of  $\rho_{\text{liq}} = 0.742$ , indicated in Fig. 4 by a dashed line. From this we would expect the segregated slow particles to develop hexagonal order at small  $z$ , which is exhibited by visual inspection by the configuration for  $z = 0.05$  in Fig. 3.

Local hexatic orientational order is measured by the parameter

$$\psi_i = \frac{1}{n_i} \sum_{j=1}^{n_i} e^{i6\theta_{ij}}, \quad (11)$$

where the sum runs over the  $n_i$  neighbors of particle  $i$ , and  $\theta_{ij}$  is the angle between  $\vec{r}_j - \vec{r}_i$  and the  $x$  axis. The spatial

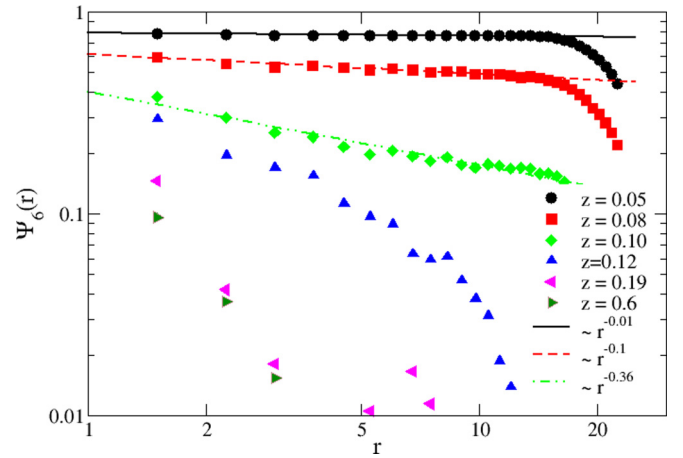


FIG. 8. Spatial correlation function of the orientational order parameter for different choices of  $z$  indicated in the legend. The lines are fits to power law decays obeyed at small  $z$ , indicating long-range orientational order. The exponents of the fits given in the legend are in the expected range [31].

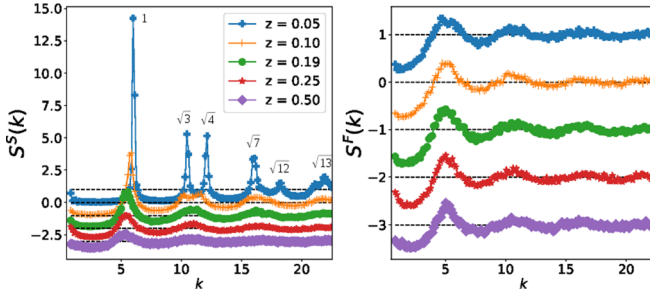


FIG. 9. Static structure factor for slow and fast particles separately as a function of the speed ratio  $z$ . Individual curves are shifted for clarity. The peak positions in the left plot follow the ratios for a hexagonal structure. The legend on the left plot is valid for both parts.

correlation function of this order parameter,

$$\Psi_6(r) = \left\langle \frac{1}{N} \sum_{i,j} \psi_i \psi_j^* \delta(r - |\vec{r}_j - \vec{r}_i|) \right\rangle, \quad (12)$$

decays exponentially in the liquid phase but with a power law in the hexatic phase. In Fig. 8 we show the behavior of the orientational correlation function for different choices of  $z$ . While this function is exponential at larger  $z$ , the decay clearly is compatible with a power law behavior at the three smallest values of  $z$  shown. In parallel to the development of orientational order, the system also develops translational order, as evidenced by the structure factor shown in Fig. 9.

Clearly, the coherent structure factor for the slow particles develops Bragg peaks upon reduction of the speed ratio (i.e., further compression of the disk of slow particles). The positions of these peaks obey ratios characteristic for a hexatic structure. In contrast, the structure factor for the fast particles remains fluidlike for all parameters. This is in line with the structures one observes at low  $z$  in Fig. 3. Taken together, Figs. 8 and 9 give a clear proof of an hexatic phase occurring below  $z = 0.1$ .

#### IV. CONCLUSIONS

We have shown here that a mixture of particles constrained to move at two fixed and distinct velocities but otherwise identical is unstable against demixing. We have shown that this occurs even if the underlying dynamics is time reversible. This generalizes the findings from a recent study [23], where the particles differed in their diffusivity. In the stochastic model by Weber *et al.*, the velocity distribution of the particles is a Gaussian with a width that differs between the two particle types. In our model, it is a two-dimensional  $\delta$  distribution with support on circles with different radii. In both cases, the difference in the momentum space distribution result in an enforced imbalance of the kinetic pressure contributions between the two components. If this imbalance is to be counteracted by the excess pressure contributions, identical particles have to demix into subsystems of different density. For our system this happens first locally and then globally. In passive systems, the lack of equilibration in momentum space is an externally imposed property of binary models. In contrast, single-species active systems self-generate this dynamically.

The dense phase of slow particles, finally, can be considered as an equilibrium system of two-dimensional repulsive disks, and we showed that it undergoes the expected liquid-to-solid transition developing hexagonal orientational and translational order. Our observations for the latter transition agree well with a recent study of the ordering transition in equilibrium two-dimensional repulsive disks.

#### ACKNOWLEDGMENTS

The authors acknowledge funding by the Alexander von Humboldt Foundation under Grant No. 3.4-IP-DEU/1135019. G.B. acknowledges financial support from CONICET (PIP 11220150100039CO) and Agencia Nacional de Promoción Científica y Tecnológica (PICT-2015-3628) (Argentina). T.S.G. acknowledges financial support from CONICET (PIP 11220150100448CO).

- [1] T. Vicsek and A. Zafeiris, *Phys. Rep.* **517**, 71 (2012).
- [2] M. C. Marchetti, J. F. Joanny, S. Ramaswamy, T. B. Liverpool, J. Prost, M. Rao, and R. A. Simha, *Rev. Mod. Phys.* **85**, 1143 (2013).
- [3] M. E. Cates and J. Tailleur, *Ann. Rev. Condens. Matter Phys.* **6**, 219 (2015).
- [4] A. Cavagna, I. Giardina, and T. Grigera, *Phys. Rep.* **728**, 1 (2018).
- [5] J. Tailleur and M. E. Cates, *Phys. Rev. Lett.* **100**, 218103 (2008).
- [6] Y. Fily and M. C. Marchetti, *Phys. Rev. Lett.* **108**, 235702 (2012).
- [7] S. C. Takatori, W. Yan, and J. F. Brady, *Phys. Rev. Lett.* **113**, 028103 (2014).
- [8] A. Wysocki, R. G. Winkler, and G. Gompper, *Europhys. Lett.* **105**, 48004 (2014).
- [9] M. C. Marchetti, Y. Fily, S. Henkes, A. Patch, and D. Yllanes, *Curr. Opin. Colloid Interface Sci.* **21**, 34 (2016).
- [10] P. Digregorio, D. Levis, A. Suma, L. F. Cugliandolo, G. Gonnella, and I. Pagonabarraga, *Phys. Rev. Lett.* **121**, 098003 (2018).
- [11] J. Bialké, H. Löwen, and T. Speck, *Europhys. Lett.* **103**, 30008 (2013).
- [12] N. D. Biniossek, H. Löwen, T. Voigtmann, and F. Smallenburg, *J. Phys.: Condens. Matter* **30**, 074001 (2018).
- [13] Y. Fily, S. Henkes, and M. C. Marchetti, *Soft Matter* **10**, 2132 (2014).
- [14] J. U. Klamser, S. C. Kapfer, and W. Krauth, *Nat. Commun.* **9**, 5045 (2018).
- [15] A. P. Solon, H. Chaté, and J. Tailleur, *Phys. Rev. Lett.* **114**, 068101 (2015).

- [16] T. Bäuerle, A. Fischer, T. Speck, and C. Bechinger, *Nat. Commun.* **9**, 3232 (2018).
- [17] F. A. Lavergne, H. Wendehenne, T. Bäuerle, and C. Bechinger, *Science* **364**, 70 (2019).
- [18] I. Buttinoni, J. Bialké, F. Kümmel, H. Löwen, C. Bechinger, and T. Speck, *Phys. Rev. Lett.* **110**, 238301 (2013).
- [19] I. Theurkauff, C. Cottin-Bizonne, J. Palacci, C. Ybert, and L. Bocquet, *Phys. Rev. Lett.* **108**, 268303 (2012).
- [20] J. Stenhammar, R. Wittkowski, D. Marenduzzo, and M. E. Cates, *Phys. Rev. Lett.* **114**, 018301 (2015).
- [21] A. P. Solon, J. Stenhammar, M. E. Cates, Y. Kafri, and J. Tailleur, *New J. Phys.* **20**, 075001 (2018).
- [22] S. C. Kapfer and W. Krauth, *Phys. Rev. Lett.* **114**, 035702 (2015).
- [23] S. N. Weber, C. A. Weber, and E. Frey, *Phys. Rev. Lett.* **116**, 058301 (2016).
- [24] L. Barberis and F. Peruani, *Phys. Rev. Lett.* **117**, 248001 (2016).
- [25] A. P. Solon, Y. Fily, A. Baskaran, M. E. Cates, Y. Kafri, M. Kardar, and J. Tailleur, *Nat. Phys.* **11**, 673 (2015).
- [26] A. P. Solon, J. Stenhammar, R. Wittkowski, M. Kardar, Y. Kafri, M. E. Cates, and J. Tailleur, *Phys. Rev. Lett.* **114**, 198301 (2015).
- [27] S. Mandal, B. Liebchen, and H. Löwen, *Phys. Rev. Lett.* **123**, 228001 (2019).
- [28] L. V. Woodcock, [arXiv:0804.0679](https://arxiv.org/abs/0804.0679).
- [29] J. Kolafa and M. Rottner, *Mol. Phys.* **104**, 3435 (2006).
- [30] B. Trefz, J. T. Siebert, T. Speck, K. Binder, and P. Virnau, *J. Chem. Phys.* **146**, 074901 (2017).
- [31] A. Hajibabaei and K. S. Kim, *Phys. Rev. E* **99**, 022145 (2019).